



CHORUS

This is the accepted manuscript made available via CHORUS. The article has been published as:

Theory of tunneling conductance and surface-state transition in superconducting topological insulators

Ai Yamakage, Keiji Yada, Masatoshi Sato, and Yukio Tanaka

Phys. Rev. B **85**, 180509 — Published 24 May 2012

DOI: [10.1103/PhysRevB.85.180509](https://doi.org/10.1103/PhysRevB.85.180509)

Theory of tunneling conductance and surface-state transition in superconducting topological insulators

Ai Yamakage,¹ Keiji Yada,¹ Masatoshi Sato,² and Yukio Tanaka¹

¹*Department of Applied Physics, Nagoya University, Nagoya 464-8603, Japan*

²*Institute for Solid State Physics, University of Tokyo, Chiba 277-8581, Japan*

(Dated: May 10, 2012)

We develop a theory of the tunneling spectroscopy for superconducting topological insulators (STIs), where the surface Andreev bound states (SABSs) appear as helical Majorana fermions. Based on the symmetry and topological nature of parent topological insulators, we find that the SABSs in the STIs have a structural transition in the energy dispersions. The transition results in a variety of Majorana fermions, by tuning the chemical potential and the effective mass of the energy band. We clarify that Majorana fermions in the vicinity of the transitions give rise to robust zero bias peaks in the tunneling conductance between normal metal/STI junctions.

PACS numbers: 74.45.+c, 74.20.Rp, 73.20.At, 03.65.Vf

Topological superconductors (TSCs) are a new state of matter^{1–3} characterized by non-zero topological numbers of the bulk wave functions. They support topologically protected gapless surface Andreev bound states (SABSs), and the superconductivity infers that the gapless SABSs are their own antiparticles, thus Majorana fermions⁴. The realization of TSC and Majorana fermions in condensed matter physics is of particular interest because of their novelty as well as the possible application for quantum devices^{5–22}.

The recent discovered superconductor $\text{Cu}_x\text{Bi}_2\text{Se}_3$ ^{23–26} is an intriguing candidate of the TSC because it is associated with another new state of matter, topological insulator: The parent material Bi_2Se_3 is originally a topological insulator with topologically protected gapless Dirac fermions on its surface. With intercalating Cu, the superconductivity appears. On the theoretical side, it has been expected that $\text{Cu}_x\text{Bi}_2\text{Se}_3$ is a TSC by the Fermi surface criterion^{27–29}, and possible SABSs specific to this material have been studied^{30–32}. Recently, a point contact spectroscopy experiment on this material has been done, and reported a zero-bias conductance peak (ZBCP)³¹. With analysis excluding other mechanisms, it has been concluded that the ZBCP is intrinsic and signifies unconventional superconductivity³¹. Moreover, similar ZBCPs have been observed by other groups independently^{33–35}.

Motivated by this finding, we develop in this Rapid Communication a general theory of Majorana fermions in superconducting topological insulators (STIs) and their relation to the tunneling conductance. Up to this time, the relation between SABSs and the tunneling conductance has been understood in quasi two-dimensional superconductors¹: (1) If the SABS has a flat band dispersion as a function of the momentum parallel to the surface, k_y , the resulting line shape of conductance always has a sharp ZBCP as realized in high- T_c cuprate^{1,36}. (2) If the SABS has a linear dispersion as a function of k_y , the resulting line shape of conductance has a broad peak as observed in Sr_2RuO_4 ^{37–39}. On the other hand, in three-dimensional superconductors, little is known about the

relation between SABSs and the tunneling conductance. The only exception is a study on the superconducting analog of superfluid ³He B phase⁴⁰. Like $\text{Cu}_x\text{Bi}_2\text{Se}_3$, it is a three dimensional TSC supporting helical Majorana fermions on its surface^{41–46}. However, the resulting tunneling conductance always shows a double-peak structure⁴⁰. Therefore, in order to pursue the origin of the observed ZBCPs in STIs, one needs to develop a theory of the tunneling conductance for STIs.

In this Rapid Communication, we study the tunneling spectroscopy and underlying SABSs in STIs. Based on symmetry and topological nature of parent topological insulators, it is shown that SABSs in STIs have a structural transition of the energy dispersion (Fig.2). The transition results in a variety of helical Majorana fermions in SABSs, which we call cone, caldera, ridge and valley. We clarify that the transition explains robustness of the ZBCP in STIs. From explicit calculation, it is found that the tunneling conductances between normal metal/STI junctions support ZBCPs near the transition. These features are proper to STIs and distinct from a simple three-dimensional TSC mentioned above. Our findings support that the observed ZBCPs in Refs.^{31,33–35} are originated from a helical Majorana fermion in STIs, and they give an evidence of their topological superconductivity. Our results are summarized in Table I.

First let us briefly review basic properties of parent topological insulators. For concreteness, we consider the following $k \cdot p$ Hamiltonian to describe the topological insulators,

$$H_{\text{TI}}(\mathbf{k}) = m\sigma_x + v_z k_z \sigma_y + v\sigma_z(k_x s_y - k_y s_x),$$

$$m = m_0 + m_1 k_z^2 + m_2(k_x^2 + k_y^2), \quad (m_1 m_2 > 0), \quad (1)$$

where s_μ and σ_μ are the Pauli matrices in spin and orbital spaces, respectively. In addition to the time-reversal symmetry, we have assumed the mirror symmetry $\mathcal{M}_i H_{\text{TI}} \mathcal{M}_i^\dagger = H_{\text{TI}}|_{k_i \rightarrow -k_i}$ with $\mathcal{M}_i = s_i$, ($i = x, y$) and the inversion symmetry. Although H_{TI} in the above is axial symmetric along the z -axis, even if one adds higher order terms of k_i ($i = x, y$) like the warping

	STI		BW
gap	full	nodal	iso
SABS	cone/caldera	ridge/valley	cone
conductance	DP/ZBP	ZBP	DP

TABLE I. Momentum-independent odd-parity pairing symmetries in STI. As a comparison, pairing symmetry in BW phase of superfluid ^3He is shown. The energy spectrum has full gap, nodal or isotropic (iso) full gap. In cases of low and intermediate transmissivity of normal metal/STI junctions, the line shapes of tunneling conductances show double peak (DP) and zero bias peak (ZBP), respectively. (see Fig.3 and the corresponding discussions in the text).

terms⁴⁷, our results do not change qualitatively. The topological phase of this system is classified by the \mathbb{Z}_2 invariant, $(-1)^\nu = \text{sgn}(m_0 m_1)$, and when \mathbb{Z}_2 non-trivial ($m_0 m_1 < 0$), the system becomes a topological insulator. On the surface perpendicular to z -axis, it supports the topologically protected Dirac fermion.

Now consider the corresponding STIs. The STIs are described by the Bogoliubov-de Gennes (BdG) Hamiltonian in the Nambu representation $(\psi_{\sigma\uparrow}, \psi_{\sigma\downarrow}, -\psi_{\sigma\downarrow}^\dagger, \psi_{\sigma\uparrow}^\dagger)$,

$$H_{\text{STI}}(\mathbf{k}) = (H_{\text{TI}}(\mathbf{k}) - \mu)\tau_z + \hat{\Delta}\tau_x, \quad (2)$$

where μ is the chemical potential, τ_μ is the Pauli matrix in the particle-hole (Nambu) space, and $\hat{\Delta}$ is a 4×4 matrix denoting the gap function. σ denotes the index of orbital. For simplicity, we assume that $\hat{\Delta}$ is a constant matrix, which is generally realized when the pairing interaction is short-range and attractive. Because of the Fermi-Dirac statistics of electrons, $\hat{\Delta}$ satisfies $\hat{\Delta} = s_y \hat{\Delta}^T s_y$, thus there are six independent pairings, $(\Delta, \Delta\sigma_x, \Delta\sigma_z, \Delta\sigma_y s_x, \Delta\sigma_y s_y, \Delta\sigma_y s_z)$ (Δ is independent of \mathbf{k}), which are introduced by Fu and Berg²⁸. For each independent pairing, we consider SABS on the surface normal to the z -axis.

In order to solve the SABS, we consider the semi-infinite STI ($z > 0$) with a flat surface at $z = 0$. The wave function in this system is given by

$$\psi_{\text{STI}}(z > 0) = \sum_I t_I u_I e^{iq_I z} e^{ik_x x} e^{ik_y y}, \quad (3)$$

where q_I ($I = 1, \dots, 8$) is a solution of $E = E(k_x, k_y, q_I)$ with $E(\mathbf{k})$ being an eigenvalue of Eq.(2), and $u_I(k_x, k_y, q_I)$ is the corresponding eigenvector. Among the eigenvectors, $\psi_{\text{STI}}(z)$ consists of those with $E(k_x, k_y, q_I)/\partial q_I > 0$ or $\text{Im}q_I > 0$, where the former denotes up-going states and the latter denotes localized states in the vicinity of $z = 0$. Postulating the boundary condition as $\psi_{\text{STI}}(z = 0) = 0$, we can determine the coefficients t_I and obtain the SABS.

Among the six pairings mentioned above, only the three $(\Delta\sigma_y s_x, \Delta\sigma_y s_y, \Delta\sigma_y s_z)$ support gapless SABSs on the surface at $z = 0$. We notice that all of them are odd-parity pairings, $P\Delta\sigma_y s_\mu P^\dagger = -\Delta\sigma_y s_\mu$, ($P = \sigma_x$), and the existence of the SABSs is consistent with the

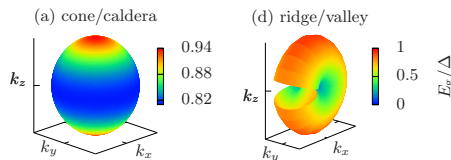


FIG. 1. (color online) Polar plots of the bulk superconducting gap E_g for full (a) and nodal (b) gaps, where cone/caldera and ridge/valley SABSs are realized, respectively. It is not plotted in a certain region for the cases (b), for visibility.

Fermi surface criterion for odd parity TSCs²⁹. Furthermore, they all are odd under (at least) one of the mirror symmetries, $\mathcal{M}_i \Delta\sigma_y s_\mu \mathcal{M}_i^\dagger = -\Delta\sigma_y s_\mu$ for $i \neq \mu$. As illustrated in Fig.1, $\Delta\sigma_y s_x$ and $\Delta\sigma_y s_y$ have point nodes in the bulk spectrum on the k_y - and k_x -axes, respectively, while $\Delta\sigma_y s_z$ is full gapped. The point nodes change a qualitative structure of the SABSs as is shown below. In the following, we focus on $\Delta\sigma_y s_z (\equiv \hat{\Delta}_f)$ and $\Delta\sigma_y s_y (\equiv \hat{\Delta}_n)$ because the result of $\Delta\sigma_y s_x$ is obtained by exchanging k_x and k_y in that of $\Delta\sigma_y s_y$.

The obtained SABSs in the STI are illustrated in Fig.2. The SABSs appear when $m_0^2 < \mu^2$. An important feature of the SABSs is that there exists a structural transition of the energy dispersion. Combined with the nodal structure mentioned above, the transition results in a variety of Majorana fermions, which we call (a) cone, (b) caldera, (c) ridge, and (d) valley: For the full gapped pairing $\hat{\Delta} = \hat{\Delta}_f$, we find that the cone and the caldera are possible. For larger values of μ and m_1 , the energy spectrum of the SABS is an axial symmetric and monotonic function of $k [\equiv (k_x^2 + k_y^2)^{1/2}]$, and its shape is a deformed cone [Fig.2(a)] including higher order terms of k . For smaller values of μ and m_1 , however, a second crossing of the zero energy appears at finite k and a *caldera* SABS is realized [Fig.2(b)]. This result is consistent with that of Refs.^{30,32}. On the other hand, for the nodal pairing $\hat{\Delta}_n$, we obtain the ridge [Fig.2(c)] and the valley [Fig.2(d)], instead. Although the structural transition occurs on the same critical line, Majorana fermions in this case have the flat dispersion due to the existence of bulk point nodes. As a result, the cone (caldera) is deformed into the ridge (valley). We can also show that the flat dispersion between the point nodes has a topological origin, thus is not accidental⁴⁸⁻⁵⁰.

Now we show that the structural transition is intrinsic to the STI. Due to an argument based on symmetry given below, we find that the STI may have a remnant of the surface Dirac fermion in the parent topological insulator, and this is the origin of the structural transition. To see this, consider how the superconductivity of $\hat{\Delta}_{g=f,n}$ may affect on the Dirac fermion. When μ is small and in the bottom of the bulk band, the surface Dirac fermion near the Fermi energy is well-separated from the bulk band. Thus, it can be treated apart, and the problem reduces to constructing a pairing term of the Dirac fermions that

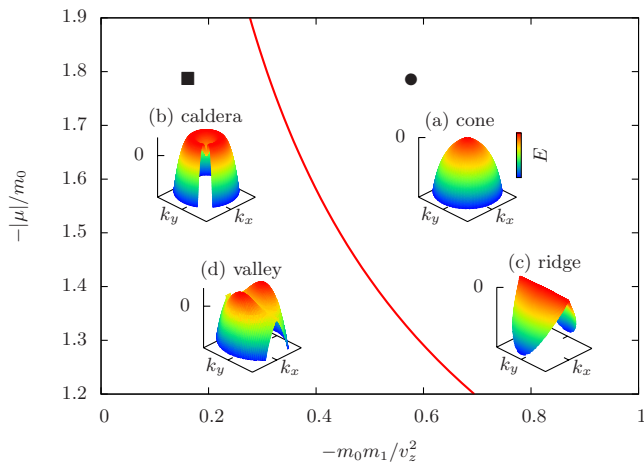


FIG. 2. (color online) Evolution of the energy dispersion of the SABS with the variation of chemical potential and $m_0 m_1$. The curve represents the boundary of parameter regions where the structure of the energy dispersion has a (a) cone [(c) ridge] or (b) caldera [(d) valley] for full (nodal) gapped pairing. The position of the circle (square) symbol corresponds to the parameters used in the calculations of tunneling conductances with $m_1 = 20.18 \text{ eV\AA}$ ($m_1 = 5.66 \text{ eV\AA}$), where a cone (caldera) or ridge (valley)-SABS is realized.

is consistent with symmetry of $\hat{\Delta}_g$. In particular, the induced pairing should have odd mirror parity as $\hat{\Delta}_g$, because the mirror symmetry \mathcal{M}_i is a good symmetry on the surface at $z = 0$. However, one find that no pairing term is allowed to be consistent with the symmetries. This means that the Dirac fermion remains to be gapless near the Fermi energy when adding $\hat{\Delta}_g$, in contrast to the case of conventional s -wave pairing^{16,51}. By hybridizing with the Majorana cone (ridge) specific to TSCs, the gapless Dirac fermion results in a caldera (valley) structure of the Majorana fermions. Now consider tuning μ deep into the bulk band. As one increases μ , the surface state near the Fermi energy merges into the bulk band, and finally disappears. One now obtains conventional Majorana cone or Majorana ridge because of no hybridization of the Dirac fermion. Therefore, a structural transition of the Majorana fermions must occur between these two limits.

We note that when the transition occurs, the velocity of the Majorana fermions at $(k_x, k_y) = 0$ changes its sign. The velocity along the x -direction \tilde{v} is given by $\tilde{v} = va\Delta/m_0$ with

$$a = \frac{1 - \sqrt{1 + 4\tilde{m}_1 + 4\tilde{m}_1^2 \tilde{\mu}^2}}{2\tilde{m}_1 \tilde{\mu}^2}, \quad (4)$$

where $\tilde{m}_1 = m_0 m_1 / v_z^2$ and $\tilde{\mu} = \mu / m_0$. The transition line determined by $a = 0$ is given by $\tilde{\mu}^2 = 1 / (-\tilde{m}_1)$, which is shown in Fig.2. Only for the case with $m_0 m_1 < 0$, the value of a can become zero, namely, topological insulator triggers the structural transition of SABS.

Now we calculate the tunneling conductance of normal metal/STI junction, generalizing theories of

the tunneling spectroscopy of conventional⁵² and unconventional^{36,53} superconductors. We suppose a free electron in the normal metal with the Hamiltonian $H_N(\mathbf{k}) = [(k_x^2 + k_y^2 + k_z^2)/(2m_e) - \mu_N]\sigma_0 s_0 \tau_z$. The wave function in the normal metal ($z < 0$) is given by

$$\psi_N(z < 0) = e^{i(k_x x + k_y y)} \left[\chi_{\sigma s e} e^{i k_{e z} z} + \sum_{\sigma' s'} (a_{\sigma s \sigma' s'} \chi_{\sigma' s' h} e^{i k_{h z} z} + b_{\sigma s \sigma' s'} \chi_{\sigma' s' e} e^{-i k_{e z} z}) \right], \quad (5)$$

where $\chi_{\sigma s \tau}$ is the eigenvector of $H_N(\mathbf{k})$ with orbital σ and spin s for electron ($\tau = e$) or hole ($\tau = h$), and $k_{e z} = \sqrt{k_e^2 - k^2} = k_e \cos \theta$, $k_e = \sqrt{2m_e(\mu_N + E)}$, $k_{h z} = \sqrt{2m_e(\mu_N - E) - k^2}$, and $a_{\sigma s \sigma' s'}$ ($b_{\sigma s \sigma' s'}$) is the Andreev (normal) reflection coefficient. The first term of the wave function denotes an injected electron, and the second (third) one denotes a reflected electron (electron) with reflection coefficient $a_{\sigma s \sigma' s'}$ ($b_{\sigma s \sigma' s'}$). On the other hand, the wave function in the STI side ($z > 0$) is given by Eq. (3) with the transmission coefficient t_I . These wave functions are connected at the interface ($z = 0$) by the condition⁵⁴, $\psi_N(0) = \psi_{\text{STI}}(0)$ and $v_N \psi_N(0) = v_{\text{STI}} \psi_{\text{STI}}(0)$, with the velocity operator $v_{N(\text{STI})} = \partial H_{N(\text{STI})} / \partial k_z |_{k_z \rightarrow -i \partial_z}$. The above equation determines the coefficients $a_{\sigma s \sigma' s'}$, $b_{\sigma s \sigma' s'}$ and t_I . Finally, the normalized charge conductance G is given by

$$\frac{G}{G_N} = \frac{\sum_{\sigma s} \int_0^{2\pi} d\phi \int_0^{\pi/2} d\theta \sin 2\theta T_{\sigma s}(\theta, \phi, eV)}{\sum_{\sigma s} \int_0^{2\pi} d\phi \int_0^{\pi/2} d\theta \sin 2\theta T_{\sigma s}(\theta, \phi, 0)|_{\Delta=0}}, \quad (6)$$

with the angle resolved transmissivity $T_{\sigma s}(\theta, \phi, E) = 1 + \sum_{\sigma' s'} (|a_{\sigma s \sigma' s'}|^2 - |b_{\sigma s \sigma' s'}|^2)$ with $k_x = k \cos \phi$, $k_y = k \sin \phi$, where the energy E of the injected electron is fixed at the bias voltage eV .

In the following, the band mass of the normal metal is fixed as $m_e m_2 = 1$ for simplicity, and we set $\Delta = 0.6 \text{ meV}$ and $\tilde{m}_1 = -0.59$ or $\tilde{m}_1 = -0.17$. The other parameters are the same as those used in Ref.³¹, i.e., $m_0 = -0.28 \text{ eV}$, $m_2 = 56.6 \text{ eV\AA}^2$, $v_z = 3.09 \text{ eV\AA}$, $v = 4.1 \text{ eV\AA}$ and $\tilde{\mu} = -1.8$. We control the transmissivity of the normal metal/STI interface by changing the value of μ_N . The transmissivity becomes maximum in this model for $\mu_N / \mu \sim 0.6$ since the magnitude of Fermi momentum in the normal metal coincides with that in STI. As μ_N increases, the magnitude of transmissivity is reduced.

The obtained tunneling conductances G/G_N near the structural transition of SABSs as functions of bias voltage eV/Δ are shown in Fig.3. With the decrease of the magnitude of transmissivity ($\mu_N / \mu = 60, 1200$), the robust ZBCPs appear stemming from the gapless SABSs in Fig.2. Only for the low transmissivity case with $\mu_N / \mu = 1200$ as shown in Fig.3 (a), G/G_N has a double-peak structure. The latter is consistent with the fact that the corresponding surface local density of states does not have a zero energy peak but double peak structure³¹. In

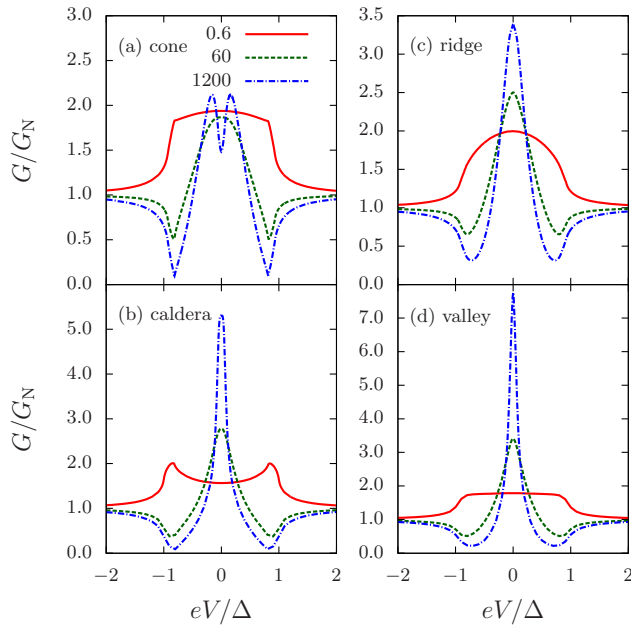


FIG. 3. (color online) The normalized tunneling conductances G/G_N near the structural transition of SABSs as functions of bias voltage eV/Δ for the cone, caldera, ridge and valley SABSs. The values denoted in the panel are of μ_N/μ_N for each line.

junctions with high transmissivity with $\mu_N/\mu = 0.6$, we obtain $G/G_N \sim 2$ for $|eV| \sim 0$ which is also consistent with the fact that an injected electron is almost perfectly reflected as a hole due to Andreev reflection.

We now focus on STI with $\hat{\Delta}_f$. It is noted that the difference of the line shapes of G/G_N between Fig.3(a) and Fig.3(b) can be understood from the different types of SABSs. In the case of Fig.3(b), a *caldera*-SABS is realized, as shown in Fig.2(b). From Eq.(4), the slope of the dispersion of the SABSs at $k = 0$ becomes gradual near the structural transition. This enhances the surface local density of states at $E = 0$ and makes the ZBCP for the tunneling conductance in the STIs. Thus the G/G_N at $eV = 0$ is enhanced in comparison with that for the cone-shaped SABS. As a result, even in the low transparent limit $\mu_N/\mu = 1200$, no double-peak structure of G/G_N appears in Fig.3(b). The present feature is different from preexisting 3D TSCs with spin-triplet p -wave pairing realized in Balian-Werthamer (BW) phase of superfluid ^3He , where in contrast to Figs. 2(a) and (b), the energy dispersion of the SABS becomes a conventional Majorana cone⁴¹⁻⁴⁶. In this case, the angle resolved transmissivity $T(\theta, \phi, eV)$ is given by

$$T(\theta, \phi, eV) = \frac{\sigma_N}{2} \sum_{s=\pm 1} \frac{1 + \sigma_N |\Gamma|^2 + (\sigma_N - 1) |\Gamma|^4}{|1 + (1 - \sigma_N) \Gamma^2 \exp(-2i\theta s)|^2}, \quad (7)$$

with the transmissivity at the interface σ_N given by $\sigma_N = 4 \cos^2 \theta / (4 \cos^2 \theta + Z^2)$ ⁵³ and $\Gamma = \Delta / (eV + \sqrt{(eV)^2 - \Delta^2})$. Z is a dimensionless constant that con-

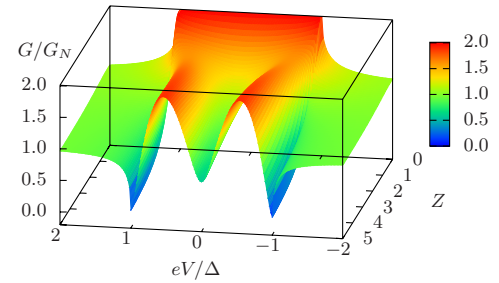


FIG. 4. (color online) The normalized tunneling conductance G/G_N as a function of bias voltage for BW state.

trols σ_N , and Δ is the superconducting gap in this system. The resulting tunneling conductance never shows a ZBCP⁴⁰ as shown in Fig.4. This difference comes from the absence of the structural transition.

Next, we consider STI with $\hat{\Delta}_n$, where the resulting SABS has a quasi-one dimensional energy dispersion. In the x -direction, SABS has a flat dispersion as mentioned before [Fig.2(c)]. The present flat dispersion of the SABS makes a ZBCP in G/G_N for arbitrary lower transmissivity, as shown in Fig.3(c). When a *valley*-cone is realized as the SABS [Fig.2(d)], G/G_N at $eV = 0$ is enhanced [Fig.3(d)].

Finally, we compare our results with the experimentally observed tunneling spectroscopy in $\text{Cu}_x\text{Bi}_2\text{Se}_3$. The tunneling conductance in $\text{Au}/\text{Ag}/\text{Cu}_{0.3}\text{Bi}_2\text{Se}_3$ junction has been observed in Ref.³¹. From the lattice constants of Au and Ag ($a \sim 4\text{\AA}$)⁵⁵, the Fermi momentum of the normal metal is estimated as $k_F \sim \pi/a \sim 1\text{\AA}^{-1}$, which corresponds to $\mu_N/\mu \sim 100$ in our model. While in the actual system, a barrier layer suppressing transmissivity could be formed between normal metal and STI, it can be taken into account as an effective increase of μ_N/μ . Therefore, the experimental result in Ref.³¹ should be compared with ours for $\mu_N/\mu > 100$. From Fig.3, we find that the experimentally observed ZBCP is consistent with $\hat{\Delta}_f$ and $\hat{\Delta}_n$, both of which support ZBCPs originating from Majorana fermions on the normal metal/STI interface.

In conclusion, we have developed a theory of the tunneling spectroscopy of STI. We have clarified the structural transition of the energy dispersion of the SABS, i.e., cone-caldera and ridge-valley transitions, which stems from remaining metallic surface states of parent topological insulator. In the vicinity of the structural transition of SABSs, even in the full-gap superconducting case, the line shapes of tunneling conductance show robust ZBCPs. On the other hand, a typical 3D topological superconductor with pair potential realized in BW phase in superfluid ^3He , never shows a ZBCP. Our obtained results serve as a guide to explore topological superconductors with Majorana fermions⁵⁶⁻⁵⁸.

ACKNOWLEDGMENTS

We thank S. Kawabata, M. Kriener, K. Segawa, S. Sasaki and Y. Ando for useful discussions. MS thanks the Kavli Institute for Theoretical Physics, UCSB, for hospitality, where this research was completed. This work was supported by MEXT (Innovative Area “Topological Quantum Phenomena” KAKENHI), and in part by the National Science Foundation under Grant No. NSF PHY05-51164.

-
- ¹ Y. Tanaka, M. Sato, and N. Nagaosa, *J. Phys. Soc. Jpn.* **81**, 011013 (2012).
- ² X.-L. Qi and S.-C. Zhang, *Rev. Mod. Phys.* **83**, 1057 (2011).
- ³ A. P. Schnyder, S. Ryu, A. Furusaki, and A. W. W. Ludwig, *Phys. Rev. B* **78**, 195125 (2008).
- ⁴ F. Wilczek, *Nature Phys.* **5**, 614 (2009).
- ⁵ M.Sato and S.Fujimoto, *Phys. Rev. B* **79**, 094504 (2009).
- ⁶ Y. Tanaka, T. Yokoyama, A. V. Balatsky, and N. Nagaosa, *Phys. Rev. B* **79**, 060505(R) (2009).
- ⁷ M.Sato, Y. Takahashi, and S. Fujimoto, *Phys. Rev. Lett.* **103**, 020401 (2009).
- ⁸ M.Sato, Y. Takahashi, and S. Fujimoto, *Phys. Rev. B* **82**, 134521 (2010).
- ⁹ M. Sato and S. Fujimoto, *Phys. Rev. Lett.* **105**, 217001 (2010).
- ¹⁰ J.D.Sau, R.M.Lutchyn, S.Tewari, and S. D. Sarma, *Phys. Rev. Lett.* **104**, 040502 (2010).
- ¹¹ J. Alicea, *Phys. Rev. B* **81**, 125318 (2010).
- ¹² R. M. Lutchyn, T. Stanescu, and S. D. Sarma, *Phys. Rev. Lett.* **105**, 077001 (2010).
- ¹³ Y. Oreg, G. Refael, and F. von Oppen, *Phys. Rev. Lett.* **105**, 177002 (2010).
- ¹⁴ R. M. Lutchyn, T. Stanescu, and S. D. Sarma, *Phys. Rev. Lett.* **106**, 127001 (2011).
- ¹⁵ J. Alicea, Y. Oreg, G. Rafael, F. von Oppen, and M. F. Fisher, *Nat. Phys.* **7**, 412 (2011).
- ¹⁶ L.Fu and C. L. Kane, *Phys. Rev. Lett.* **100**, 096407 (2008).
- ¹⁷ L. Fu and C. L. Kane, *Phys. Rev. Lett.* **102**, 216403 (2009).
- ¹⁸ A. R. Akhmerov, J. Nilsson, and C. W. J. Beenakker, *Phys. Rev. Lett.* **102**, 216404 (2009).
- ¹⁹ K. T. Law, P. A. Lee, and T. K. Ng, *Phys. Rev. Lett.* **103**, 237001 (2009).
- ²⁰ Y. Tanaka, T. Yokoyama, and N. Nagaosa, *Phys. Rev. Lett.* **103**, 107002 (2009).
- ²¹ J. Linder, Y. Tanaka, T. Yokoyama, A. Sudbo, and N. Nagaosa, *Phys. Rev. Lett.* **104**, 067001 (2010).
- ²² A. Yamakage, Y. Tanaka, and N. Nagaosa, *Phys. Rev. Lett.* **108**, 087003 (2012).
- ²³ Y. S. Hor, A. J. Williams, J. G. Checkelsky, P. Roushan, J. Seo, Q. Xu, H. W. Zandbergen, A. Yazdani, N. P. Ong, and R. J. Cava, *Phys. Rev. Lett.* **104**, 057001 (2010).
- ²⁴ L. A. Wray, S.-Y. Xu, Y. Xia, Y. S. Hor, D. Qian, A. V. Fedorov, H. Lin, A. Bansil, R. J. Cava, and M. Z. Hasan, *Nature Phys.* **6**, 855 (2010).
- ²⁵ M. Kriener, K. Segawa, Z. Ren, S. Sasaki, and Y. Ando, *Phys. Rev. Lett.* **106**, 127004 (2011).
- ²⁶ M. Kriener, K. Segawa, Z. Ren, S. Sasaki, S. Wada, S. Kuwabata, and Y. Ando, *Phys. Rev. B* **84**, 054513 (2011).
- ²⁷ M. Sato, *Phys. Rev. B* **79**, 214526 (2009).
- ²⁸ L. Fu and E. Berg, *Phys. Rev. Lett.* **105**, 097001 (2010).
- ²⁹ M. Sato, *Phys. Rev. B* **81**, 220504(R) (2010).
- ³⁰ L. Hao and T. K. Lee, *Phys. Rev. B* **83**, 134516 (2011).
- ³¹ S. Sasaki, M. Kriener, K. Segawa, K. Yada, Y. Tanaka, M. Sato, and Y. Ando, *Phys. Rev. Lett.* **107**, 217001 (2011).
- ³² T. H. Hsieh and L. Fu, *Phys. Rev. Lett.* **108**, 107005 (2012).
- ³³ T. Kirzhner, E. Lahoud, K. Chaska, Z. Salman, and A. Kanigel, arXiv:1111.5805.
- ³⁴ G. Koren, T. Kirzhner, E. Lahoud, K. B. Chashka, and A. Kanigel, *Phys. Rev. B* **84**, 224521 (2011).
- ³⁵ F. Yang, Y. Ding, F. Qu, J. Shen, J. Chen, Z. Wei, Z. Ji, G. Liu, J. Fan, C. Yang, T. Xiang, and L. Lu, *Phys. Rev. B* **85**, 104508 (2012).
- ³⁶ Y. Tanaka and S. Kashiwaya, *Phys. Rev. Lett.* **74**, 3451 (1995).
- ³⁷ C. Honerkamp and M. Sigrist, *J. Low Temp. Phys.* **111**, 895 (1998).
- ³⁸ M. Yamashiro, Y. Tanaka, and S. Kashiwaya, *Phys. Rev. B* **56**, 7847 (1997).
- ³⁹ S. Kashiwaya, H. Kashiwaya, H. Kambara, T. Furuta, H. Yaguchi, Y. Tanaka, and Y. Maeno, *Phys. Rev. Lett.* **107**, 077003 (2011).
- ⁴⁰ Y. Asano, Y. Tanaka, Y. Matsuda, and S. Kashiwaya, *Phys. Rev. B* **68**, 184506 (2003).
- ⁴¹ X. L. Qi, T. L. Hughes, S. Raghu, and S. C. Zhang, *Phys. Rev. Lett.* **102**, 187001 (2009).
- ⁴² A. P. Schnyder, S. Ryu, A. Furusaki, and A. W. W. Ludwig, *Phys. Rev. B* **78**, 195125 (2008).
- ⁴³ Y. Nagato, S. Higashitani, and K. Nagai, *J. Phys. Soc. Jpn.* **78**, 123603 (2009).
- ⁴⁴ G. Volovik, *JETP Lett.* **90**, 587 (2009).
- ⁴⁵ G. Volovik, *JETP Lett.* **90**, 398 (2009).
- ⁴⁶ Y. Tsutsumi, M. Ichioka, and K. Machida, *Phys. Rev. B* **83**, 094510 (2011).
- ⁴⁷ L. Fu, *Phys. Rev. Lett.* **103**, 266801 (2009).
- ⁴⁸ K. Yada, M. Sato, Y. Tanaka, and T. Yokoyama, *Phys. Rev. B* **83**, 064505 (2011).
- ⁴⁹ M. Sato, Y. Tanaka, K. Yada, and T. Yokoyama, *Phys. Rev. B* **83**, 224511 (2011).
- ⁵⁰ Y. Tanaka, Y. Mizuno, T. Yokoyama, K. Yada, and M. Sato, *Phys. Rev. Lett.* **105**, 097002 (2010).
- ⁵¹ M.Sato, *Phys. Lett. B* **575**, 126 (2003).
- ⁵² G. E. Blonder, M. Tinkham, and T. M. Klapwijk, *Phys. Rev. B* **25**, 4515 (1982).
- ⁵³ S. Kashiwaya and Y. Tanaka, *Rep. Prg. Phys.* **63**, 1641 (2000).
- ⁵⁴ L. W. Molenkamp, G. Schmidt, and G. E. W. Bauer, *Phys. Rev. B* **64**, 121202 (2001).
- ⁵⁵ N. W. Ashcroft and N. D. Mermin, *Solid State Physics* (Saunders College, Philadelphia, 1976).
- ⁵⁶ A. P. Schnyder, P. M. R. Brydon, D. Manske, and C. Timm, *Phys. Rev. B* **82**, 184508 (2010).
- ⁵⁷ A. P. Schnyder, P. M. R. Brydon, and C. Timm, *Phys. Rev. B* **85**, 024522 (2012).
- ⁵⁸ S. Nakosai, Y. Tanaka, and N. Nagaosa, *Phys. Rev. Lett.* **108**, 147003 (2012).